Magazine of Civil Engineering

ISSN 2712-8172

journal homepage: http://engstroy.spbstu.ru/

Research article

UDC 691.3

DOI: 10.34910/MCE.123.5

Cementless binder consisting of high-calcium fly ash, silica fume and magnesium chloride

K. Usanova[1] ✉, ***Yu.G. Barabanshchikov***[1], ***S. Dixit*** [2, 3, 4]

[1] *Peter the Great St. Petersburg Polytechnic University, St. Petersburg, Russian Federation*

[2] *Division of Research, Uttaranchal University, Dehradun, India*

[3] *Division of Research and Development, Lovely Professional University, Phagwara, Punjab, India*

[4] *Khalifa University, Abu Dhabi, United Arab Emirates*

✉ *plml@mail.ru*

Keywords: fly ash, microsilica, silica fume, early strength agent, $MgCl_2$, X-ray diffraction analysis, strength, heat release, differential thermal analysis, heat of hydration, phase composition

Abstract. This work aims to study the effect of $MgCl_2$ additive on the strength, heat of hydration, and phase composition of hydration products of the binder consisting of high-calcium fly ash and silica fume. Fly ash from Berezovskaya thermal power plant, containing a lot of CaO_{free}, in combination with silica fume does not expand and exhibits the properties of a binder. However, the strength of this binder is low. The $MgCl_2$ additive significantly increases the hardening rate and the final strength of the mix. The compressive strength of 32×32×32 mm specimens from the paste at the age of 7 days is 15.2 MPa and 3.7 MPa with and without the $MgCl_2$ additive, respectively. Exothermic data show that silica fume inhibits CaO hydration from the first minutes of the reaction to 2 days, after which the process accelerates and proceeds evenly. The total value of the thermal effect for 10 days is 500 kJ per 1 kg of binder. The $MgCl_2$ additive does not increase this final value, however, it accelerates the release of heat in the initial periods, excluding the indicated stagnation period. The results of XRD and DTA showed that in the presence of $MgCl_2$, calcium hydrochloraluminate (Friedel's salt) is formed, which was not previously observed in the composition of binder hydration products.

Funding: Russian Science Foundation grant No. 21-19-00324, https://rscf.ru/project/21-19-00324/

Citation: Usanova, K., Barabanshchikov, Yu.G., Dixit, S. Cementless binder consisting of high-calcium fly ash, silica fume and magnesium chloride. Magazine of Civil Engineering. 2023. 123(7). Article no. 12305. DOI: 10.34910/MCE.123.5

1. Introduction

Fly ash is a finely dispersed material generated from the combustion of coal in thermal power plants. Numerous theoretical and practical studies, as well as world experience, show that industrial waste is a suitable raw material for replacing natural resources in the construction industry [1–4]. Fly ash is actively used in the concrete production as an additive [5–7], as a partial replacement for cement [8–10], as an artificial aggregate [11, 12] and as a binder for the production of geopolymers [13, 14]. A well-known solution is also the use of fly ash to obtain cementless binders [15, 16].

The fly ash properties directly depend on the type of coal burned. Combustion of anthracite or bituminous coals produces fly ash with a low CaO content. This fly ash is class F according to International Standard Specification ASTM C618. The combustion of brown coal produces fly ash with a CaO content of more than 10 %. This fly ash is class C according to ASTM C618.

The use of class C fly ash with a high content of CaO_{free} in concrete technology leads to a strong expansion and cracking of the material during the curing period. This prevents the use of high calcium fly ash in concrete production [17–19].

There are known methods for neutralizing the high calcium fly ash expansion in blended binders consisting of fly ash and cement. The silica fume additive in the dry mix causes shrinkage, which minimizes expansion and thus reduces crack development [20–22]. Another solution for neutralizing CaO_{free} is the co-grinding and hydrolysis of fly ash [23, 24]. It is possible to contain the expansion of dough from cement and fly ash by adding carbon fiber [25] or alkali-resistant glass fiber [26, 27].

The following ways to neutralize the expansion of a binder based only on high-calcium fly ash are known: pre-hydration, which reduces the amount of ettringite [28, 29], grinding, which accelerates the anhydrite and lime hydration [30], and cavitation technology [31].

The easiest way to neutralize fly ash expansion is to use silica fume additives. The study [32] proves the silica fume effectiveness in relation to the expansion of high-calcium fly ash from Berezovskaya thermal power plant during hydration. Expansion and cracking of the fly ash can be completely prevented by adding about 40 % microsilica to the fly ash. Such mixes do not have high strength [32]; therefore, they require the selection of hardening-accelerating admixture.

Chloride early strength agents are widely used in cement-based materials [33, 34]. Studies [35, 36] have shown that a certain amount of chlorides can effectively shorten the setting time of cement-based materials and improve the early strength.

The authors [37] studied the composition of waste rock, fly ash and cement in a ratio of 5:3:1 with the addition of chloride early strength agents. It found that NaCl and $CaCl_2$ promote early setting, while $MgCl_2$ reduces setting speed. The hydration heat increases if NaCl and $CaCl_2$ are used, but the hydration heat decreases if the addition of $MgCl_2$ is used.

Using chloride agents may cause reinforcement corrosion [38, 39]. It is known that free chloride ion moves inside the concrete and reduces the alkalinity of the pore solution, which causes decontamination and corrosion of the reinforcing steel in concrete [40]. But at the same time, the fixed chloride ion can react with $Ca(OH)_2$ and C_3A and form Friedel's salt ($C_3A{\cdot}CaCl_2{\cdot}10H_2O$), and the higher the chloride content in the solution, the more Friedel's salt will be generated [41, 42]. At the initial curing stage, Friedel's salt can effectively fill the gap between aggregates and improve the mechanical strength of the material [37].

Thus, the use of chloride agents in binders consisting of high-calcium fly ash and silica fume should reduce the content of free chloride ions by increasing the content of fixed chloride ions. In this case, the use of such a composition in concrete technology will be quite wide, for example, in the form of a cementless binder or in granular form, as a coarse aggregate of concrete.

The object of study is blended binders consisting of high-calcium fly ash from Berezovskaya thermal power plant and silica fume additive.

The work aims to study the effect of $MgCl_2$ additive on the strength, heat of hydration, and phase composition of hydration products of the binder based on high-calcium fly ash and silica fume.

Tasks of the research:

1. Experimental study of various early strength agents on their ability not to cause expansion in the composition of the cementless binder, consisting of high-calcium fly ash and silica fume.

2. Determination based on the results of X-ray Diffraction Analysis (XRD) what interactions occur in the "fly ash – silica fume – $MgCl_2$" system and how how these interactions affect the hydration.

3. Differential Thermal Analysis (DTA) of cementless binder specimens with different content of $MgCl_2$ additive.

4. Experimental study of the $MgCl_2$ additive on the heat release of cementless binder.

5. Experimental study of the effect of the $MgCl_2$ additive on the compressive strength of specimens from a mortar with polyfraction standard sand.

2. Materials and Methods

2.1. Materials

1. High-calcium fly ash from Berezovskaya thermal power plant (Krasnoyarsk Territory, Russia). The chemical composition of the tested specimens of fly ash is given in Table 1 [32].

Table 1. Chemical composition of fly ash.

CaO	SiO_2	Al_2O_3	Fe_2O_3	MgO	P_2O_5	SO_3	K_2O	Na_2O	Chlorine ion	C	Loss on ignition
42.2	26.8	6.49	6.09	7.05	<0.1	2.86	0.23	0.43	<0.05	2.33	3.44

The chemical composition of fly ash from the coal combustion of the Berezovsky deposit is characterized by a high content of CaOfree, which is 15.4 %. Fly ash from coals of the Berezovsky deposit is mineralogically represented mainly by silicates, aluminosilicates, and calcium ferrites, as well as calcium, magnesium and aluminium oxides (Table 2). Small amounts of TiO_2, MnO_2, and P_2O_5 are also present. Minerals such as brownmillerite, andradite, merwinite, grossular, and quartz are also identified. It should be noted that the fly ash contains a significant amount of unburned carbonaceous particles.

Fly ash from Berezovskaya thermal power plant sets and hardens when mixed with water. However, due to the presence of a large amount of free lime, its hardening is accompanied by strong expansion and cracking.

Table 2. Composition of fly ash according to X-ray diffraction analysis.

Crystal phases	Chemical Compound	Conditional Content [%]
Lime	Ca O	62.39
Graphite	C	12.81
Periclase	Mg O	7.3
Brownmillerite	$4CaO{\cdot}Al_2O_3{\cdot}\ Fe_2O_3$	3.71
Andradite	$3CaO{\cdot}Fe_2O_3{\cdot}3SiO_2$	3.62
Merwinite	$3CaO{\cdot}MgO{\cdot}2SiO_2$	3.39
Millosevichite	$Al_2(SO_4)_3$	1.97
Calcium Aluminum Oxide	$3CaO{\cdot}Al_2O_3$	1.92
Grossular	$3CaO{\cdot}Al_2O_3{\cdot}3SiO_2$	1.06
Aluminum Oxide	Al_2O_3	0.54
Yeelimite	$3CaO{\cdot}Al_2O_3{\cdot}CaSO_4$	0.51
Kilchoanite	$3CaO{\cdot}2SiO_2$	0.41
Quartz	SiO_2	0.38

The corresponding X-ray diffraction pattern is shown in Fig. 1.

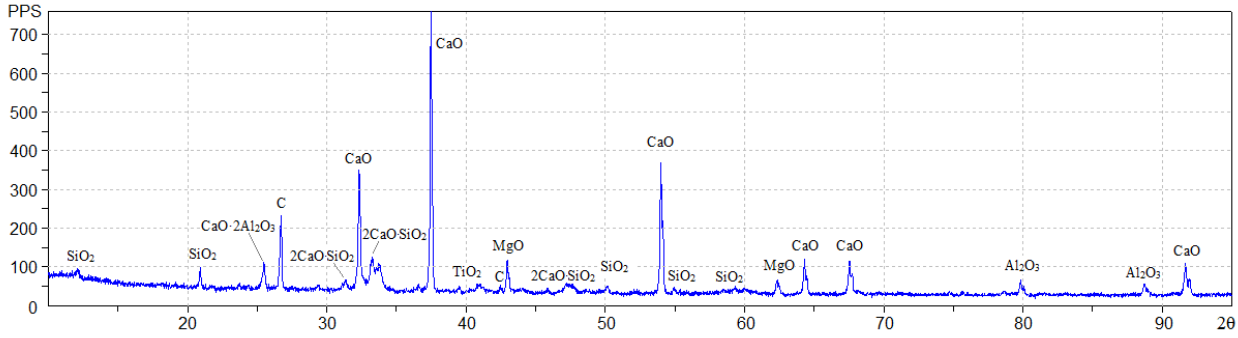

Figure 1. X-ray diffraction pattern of fly ash.

2. Silica Fume MKU-85. The additive is used to neutralize the expansion of fly ash.

3. Early strength agents: Al_2O_3, $Ca(OH)_2$, $CaCl_2$, Na_2SO_4, $MgSO_4$, K_2O, $MgCl_2$. Early strength agents are used to select an additive that increases the strength and water resistance of the binder, consisting of

fly ash from Berezovskaya thermal power plant and silica fume. The content of early strength agents and silica fume (MS) by weight of fly ash are presented in Table 3.

Table 3. Content of early strength agents and silica fume (MS) by weight of fly ash.

Type of additives	Al_2O_3	$Ca(OH)_2$	$CaCl_2$	Na_2SO_4	$MgSO_4$	K_2O	$MgCl_2$
Accelerator additive content [%]	21.4	21.2	7.0	11.5	11.5	7.7	12.2
MS content [%]	21.4	21.2	42.9	42.3	42.3	42.5	42.5
Water-fly ash ratio W/A	0.71	0.77	0.71	0.70	0.85	0.93	0.90

2.2. Influence of early strength agents on fly ash expansion in presence of silica fume

Expansion tests were carried out using Le Chatelier molds. Fly ash in the amount of 50 g, silica fume and early strength agents in the amount from Table 3 were taken for one Le Chatelier molds. First, the dry mixture was mixed by hand, and then water was slowly added until the consistency of all compositions was the same. The tests were carried out in accordance with EN 196-3:2016 Test Methods for Cement, Part 3: Determination of setting time and strength. Le Chatelier molds were placed on glass plates and filled with fly ash paste with additives in one go without compaction. Excess paste is cut off. Forms were covered from above with plates weighing 100 g and cured in air. The temperature was 20 ± 2 °C, relative air humidity was 45–55%. Unlike EN 196-3:2016, the samples were not boiled. The distance f between the ends of indicator arms was periodically measured with a caliper with an accuracy of 0.5 mm, and the difference $\Delta f = f - d$ was calculated, where d is the distance before the experiment.

2.3. Determination of compressive strength of specimens with early strength agents

The compressive strength was determined on specimens of a cubic shape with size of 32×32×32 mm. A total of 12 compositions based on a dry mixture of fly ash and silica fume in an amount of 30.4 % by weight of the fly ash were tested. The compositions differed in the type of early strength agents and their content. According to the results of testing the compositions in Le Chatelier moulds, three type of the early strength agents were selected with an expansion Δf < 5 mm: $MgSO_4$, $CaCl_2$ and $MgCl_2$. Each of the additives was used in four dosages: 1.5; 4.7; 8.2; 11.8 % by weight of fly ash. Early strength agents were introduced into the mixture in the form of an aqueous solution. The water content of the solution was considered in the calculation of the water/solid ratio (W/S). The water content in the finished mixture was selected so as to obtain mixtures with the same consistency. Therefore, the value of W/S was a characteristic of the water demand of the fly ash. 6 specimens of each composition were prepared. Demoulding of the specimens was carried out after 2 days. Immediately after demoulding, three out of 6 specimens were placed in water, and the other three were left to harden in sealed containers, which did not allow the specimens to dry out and exclude their contact with the outside air in a laboratory room with a temperature of 20 ± 2 °C. Specimens of both dry and wet hardening were tested for compressive strength after 7 days from the date of manufacture. Before testing, the state of the specimens was visually assessed, the presence of expansion and cracks.

2.4. X-ray Diffraction Analysis and Differential Thermal Analysis

The use of X-ray diffraction analysis and differential thermal analysis was aimed at establishing what interactions occur in the fly ash–silica fume–$MgCl_2$ system and how these interactions were related to expansion. XRD and DTA were performed on specimens of the mixes listed in Table 4.

Table 4. Compositions of paste.

Component	Components content in the composition of blended binder [%]		
	Mix 1	Mix 2	Mix 3
Fly ash from Berezovskaya TPP	100	70	64.7
Silica Fume MKU-85	-	30	27.7
$MgCl_2$	-	-	7.6
Water-solid ratio W/S	1.2	0.42	0.50

Specimens for XRD and DTA were prepared as follows. First, fly ash and silica fume were mixed in an automatic mortar mixer for 6 minutes, then the calculated amount of $MgCl_2$ solution with a density of 1.24 g/cm^3 and water were added, considering the amount of water in the additive solution. Specimens were stored above water in a closed container. After the end of the curing period, the specimens were crushed before passing through a sieve with mesh 0.25 mm and subjected to vacuum drying for 3 hours at a residual pressure of 3.3 Pa. The dried specimens were ground in an agate mortar until they passed through a 005 sieve.

Semiquantitative analysis of crystalline phases in the specimens was carried out on a Dron 7 X-ray diffractometer produced by JSC"E" Burevestnik"(Russia) with the following parameters: CuKα radiation, λ = 0.15406 Å, 2θ shooting range from 8° to 94° with a step of 0.02°, and an exposure of 3 and 5 s.

Differential thermal analysis was performed on the device"Termoscan-" produced by LLC"Analitpribo" (Russia). The specimens for DTA had a mass of about 0.7–0.8 g. The specimens were heated to a temperature of 950–1000 °C.

2.5. Heat of Hydration of mortar using Semi-Adiabatic Calorimetry

The test was carried out in accordance with EN 196-9:2010"Methods of testing cement part 9: heat of hydration—semi-adiabatic method".

The paste was placed in a thin-walled aluminum container and in a glass Dewar flask. A hot junction of a differential thermocouple and a control thermometer were placed in the center of the specimen reservoir. To determine the heat capacity, the specimen was supplied with an electric heater in the form of an insulated nichrome wire wound around the cylindrical surface of the specimen reservoir. The Dewar flask with a specimen, closed with a polystyrene foam stopper, with heater and thermocouple wires, was placed in the center of a heat-insulated thermostat case. To regulate the air temperature in the thermostat, it was equipped with a cooling device and a fan. During the experiments, the temperature of the air surrounding the thermos was maintained constant using a contact thermometer and an electronic thermostat. Fluctuations in the temperature of the medium relative to the average value were ±0.3 °C. Specimen temperature was recorded automatically every 30 min with an accuracy of 0.1 °C. The thermocouple readings were recorded by a"Terem-" multi-channel data logger every 30 minutes.

When measuring the exotherm of the specimen, the heating element was not used or was absent.

To obtain comparable results, the heat of hydration obtained by the semi-adiabatic method at an initial specimens temperature of 20 °C was recalculated to an isothermal hardening regime at a temperature of 20 °C using the reduced time hypothesis [43].

The heat of hydration was determined in the mix consisting of fly ash, silica fume, early strength agents and polyfraction standard sand on cylindrical specimens with diameter of 62 mm, high of 160 mm. Three mix of the mortar were tested (mixes Q1, Q4, Q5) with the same amount of fly ash, but with a different combination of additives (Table 5).

Table 5. Mixes and designation of specimens for determining heat of hydration and strength

Component	Material Consumption [kg/m^3]		
	Q1	Q4	Q5
Fly ash from Berezovskaya TPP	210	210	210
Silica fume MKU-85	-	90 (42.9 %)	90 (42.9 %)
$MgCl_2$ (dry)	-	-	24.8 (11.8 %)
Polyfraction standard sand	1645	1476	1451
Water	318	340	330
Total	2173	2116	2106

3. Results and Discussion

3.1. Evaluation of influence of early strength agents

The test results of early strength agents (Table 3) are shown in Fig. 2.

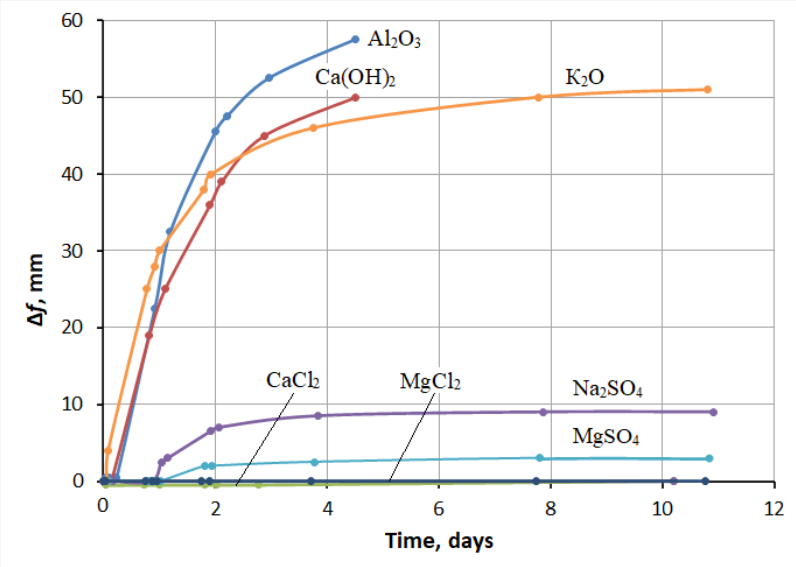

Figure. 2. Influence of early strength agents in complex with silica fume (MS) on fly ash paste expansion.

The high expansion of specimens with additives of Al_2O_3, $Ca(OH)_2$, K_2O is possibly associated with silica fume neutralization reactions, with the formation of $Al_2(SiO_3)_3$ in the case of aluminum oxide and MS, and with the formation of potassium and calcium hydrosilicates in the other two cases.

Additions of chloride and sulfate salts showed good results. Fly ash expansion with these additives was within the normal range for cement (10 mm). Chlorides showed a particularly high effect; expansion was almost non-existent. As shown below, this effect of chlorides was also retained during the aqueous exposure of the specimens. In connection with the action of these salts, it can be assumed that the specimen's expansion, especially during hardening in water, was caused by ettringite formation. Since it is known that the presence of chlorides slows down or stops the concrete expansion under the action of sulfate solutions. This is due to an increase in the solubility of calcium hydrosulfoaluminate in chloride solutions. However, X-ray diffraction analysis did not show the presence of significant amounts of ettringite in the hydration products. Therefore, the free lime hydration process was responsible for the expansion.

3.2. Compressive Strength and Water Resistance Test Results

The test results of specimens consisting of fly ash, MS, and early strength agents are presented in Table 6.

Table 6. Compressive strength (MPa).

Type of early strength agent		$MgSO_4$		$CaCl_2$		$MgCl_2$	
Curing		dry	water	dry	water	dry	water
Early strength agent content, % by weight of fly ash	1.5	8.2	0	5.8	0	2.9	0
	4.7	6.1	2.7	8.8	0	8.3	0
	8.2	4.4	1.2	7.9	1.53	9.8	1.92
	11.7	5	1.2	4.6	1.15	15.2	2.3

The strength of specimens with $MgSO_4$ decreased with increasing additive. The specimens hardened in water underwent significant expansion and cracking. When specimens hardened in dry conditions, these phenomena did not occur. The highest strength of 8.2 MPa was shown by specimens with a $MgSO_4$ content of 1.5 %.

Calcium chloride at dosages of 8.2 and 11.8 % caused a rapid thickening of the mix. As a result, the strength of these specimens was low. At the same time, these specimens did not have cracks and expansion during water hardening, in contrast to specimens with a lower $CaCl_2$ content. All specimens retained their shape and continuity under air conditions. The strength of dry hardening specimens with CaCl2 content of 4.7 % was the highest and amounted to 8.8 MPa; however, such specimens crumbled in water.

The $MgCl_2$ additive showed a relatively good result in compressing specimens hardened in dry conditions. The strength at an additive content of 11.8 % was 15.2 MPa. However, the strength dropped sharply to 2.3 MPa (Table 6) during the water hardening of specimens.

The appearance of specimens with $MgCl_2$ additive is shown in Fig. 3. It can be seen that the dry hardening specimens with a low content of magnesium chloride (1.5 %) underwent cracking. In water, specimens of this mix blurred, forming a liquid-like mass. Specimens with a high content of $MgCl_2$ (8.2–11.8 %) passed the test without cracking, both in air and in water; however, there was a slight expansion of the specimens in water. Since $MgCl_2$ is the best solution at this stage, we continued researching this supplement.

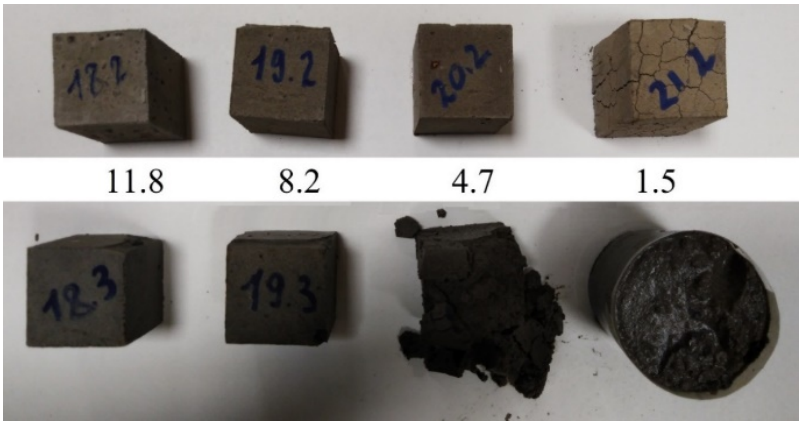

Figure 3. Specimens from fly ash, MS, and $MgCl_2$ additive in amount indicated in photo in % by weight of fly ash. Top row is with dry curing; bottom row is water curing.

3.3. Influence of magnesium chloride on phase composition of hydration products of binder

3.3.1. Results of X-ray diffraction analysis

X-ray patterns of specimens consisting of fly ash, silica fume (MS), and the $MgCl_2$ additive of mixes 1-3 (Table 4) after hydration are shown in Fig. 4, 5.

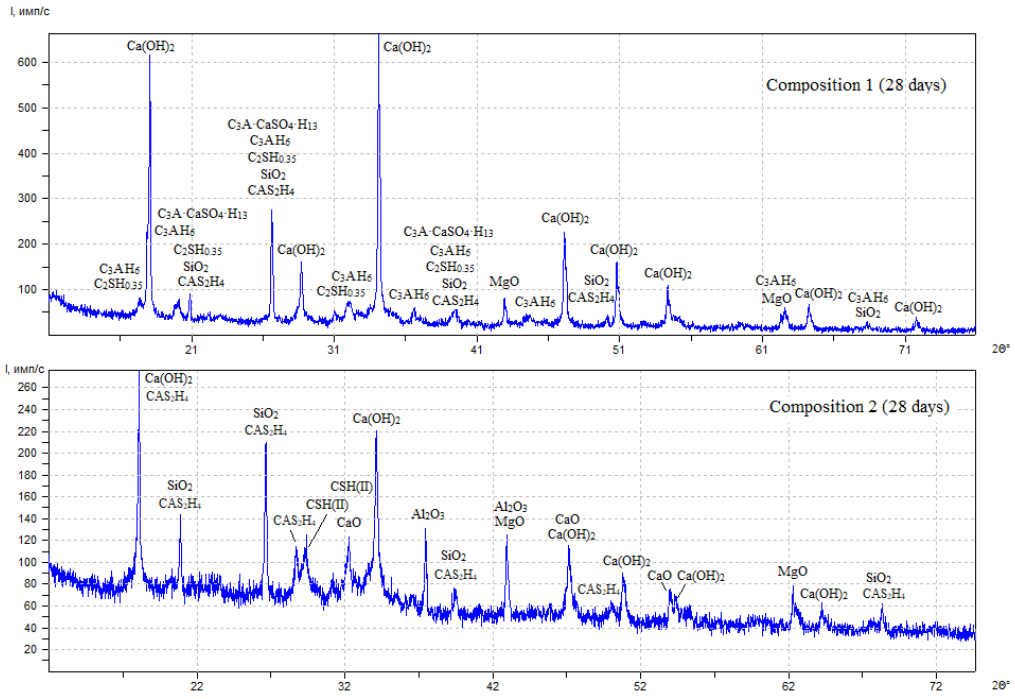

Figure 4. X-ray patterns of mixes 1 and 2 (Table 4) after hydration at age of 28 days.

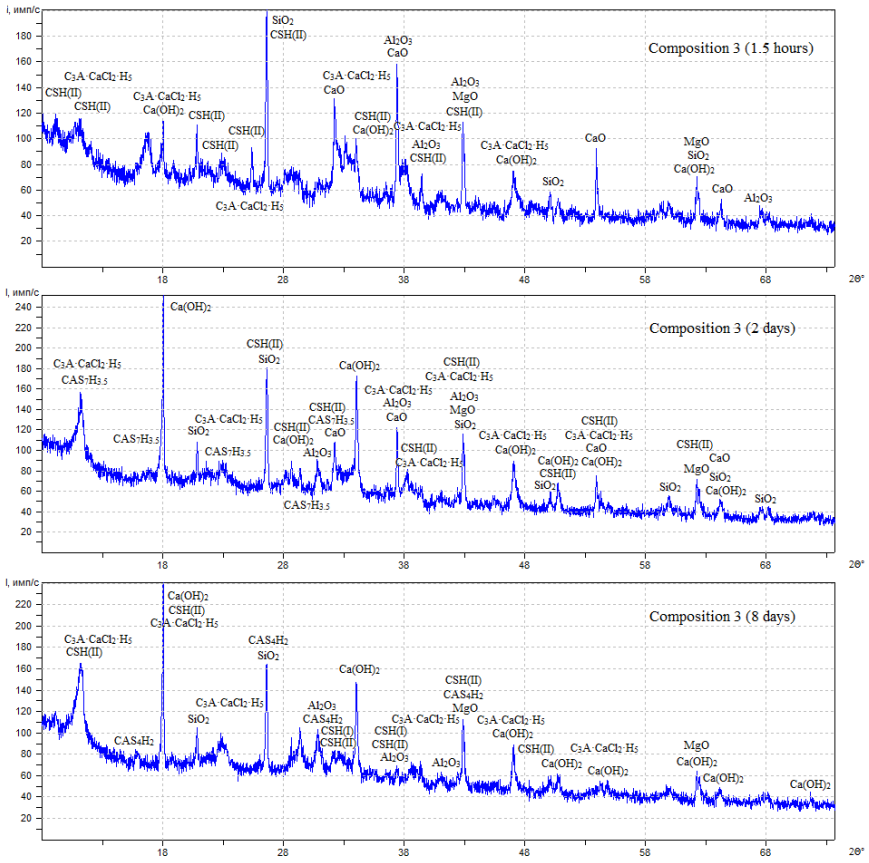

Figure 5. X-ray patterns of mix 3 (Table 4) after hydration at age of 1,5 hour, 2 days, and 8 days.

A semiquantitative analysis was carried out using the integral values of the intensity of the X-ray peaks. The obtained conditional values of the percentage of identified hydrated phases are given in Table 7.

Table 7. Crystalline phases of fly ash.

Phases	Chemical Compound	Mix 1 (28 days)	Mix 2 (28 days)	Mix 3		
				1.5 hours	2 days	8 days
Lime	CaO	-	12.8	27,3	10.8	-
Portlandite	$Ca(OH)_2$	85.4	41.8	12,5	32.3	34.1
Katoite	C_3AH_6	11.1	-	-	-	-
Calcium Aluminum Oxide Hydrate	C_4AH_{19}	-	-	-	5.6	-
Hydrocalumite	C_4AH_{13}	-	-	-	10.4	20.0
Gismondine	CAS_2H_4	-	27.5	40,2	18.9	25.4
Calcium Aluminum Silicate Hydrates	CAS_4H_2	-	-	-	-	3.2
Katoite silication	C_3ASH_4	-	2.7	-	6.2	
Calcium Silicate Hydrates	CSH(II)	-	15.2	-	1.6	2.1
Calcium Aluminum Oxide Sulfate Hydrate	$C_3A{\cdot}CaSO_4{\cdot}H_{13}$	3.5	-	-	-	-
Calcium Aluminum Oxide Chloride Hydrate	$C_3A{\cdot}CaCl_2{\cdot}H_{10}$	-	-	20.0	14.1	15.1

The following conclusions can be drawn from the data in Table 7.

1. In the absence of silica fume and $MgCl_2$ (mix 1), the interaction of fly ash with water for 28 days leads to the complete hydration of CaO_{free}. At the same time, calcium hydroxide is formed in an overwhelming amount from the hydration products of 85.4 % of the specimen's mass. Hydrosilicates in crystalline form are not found. There is C_3AH_6 (11.1 %) from calcium hydroaluminates. A small proportion (3.5 %) is the low sulfate form of calcium hydrosulfoaluminate.

2. The addition of silica fume to the fly ash (mix 2) slows down the hydration of the lime. This corresponds to the effect of siliceous admixture on the slaking rate of air-hardening lime. After 28 days of hydration, a significant amount of unreacted CaO_{free} (20.6 %) remains in the fly ash, and the content of $Ca(OH)_2$ is almost halved compared to mix 1, apparently as a result of the action of silica fume, as indicated by the significant content of the formed silicates and calcium aluminosilicates. The effect of silica fume on the hydration of high-calcium fly ash was considered by us in more detail in [32].

3. The effect of $MgCl_2$ (Mix 3) was investigated for three hydration periods. After 1.5 hours, a significant amount of unreacted CaO_{free} (36 %) and a small amount of $Ca(OH)_2$ remain in the mix. Calcium hydrosilicates are completely absent, which is explained by the short time for reactions and crystallization of hydration products. In subsequent periods, the content of lime decreases, and by 8 days, it is completely bound into hydrates, aluminates, and calcium aluminosilicates, which make up a significant proportion of the total number of neoplasms. Silicates are present in negligible quantities. Based on these data, it can be concluded that $MgCl_2$ accelerates the hydration of lime and its binding to silica. At the same time, the addition of magnesium chloride intensifies the formation of crystalline hydrates of calcium aluminosilicates, and hydrosilicates are formed to a greater extent in the X-ray amorphous state.

4. In the presence of $MgCl_2$, a new compound is found that has not previously appeared in the composition of hydration products; this is calcium hydrochloraluminate (Friedel's salt).

The content of Friedel's salt changes little with the age of the specimens. Friedel's salt here can be formed as a result of the replacement of sulfate ions in $C_3A{\cdot}CaSO_4{\cdot}H_{13}$, found in mix 1, with chloride ions:

$$2Cl^- + 3CaO{\cdot}Al_2O_3{\cdot}CaSO_4{\cdot}13H_2O \rightarrow 3CaO{\cdot}Al_2O_3{\cdot}CaCl_2{\cdot}10H_2O + SO_4^{2-} + 3H_2O,$$

or when interacting with tricalcium hydroaluminate

$$3CaO{\cdot}Al_2O_3{\cdot}6H_2O + MgCl_2 + Ca(OH)_2 + 4H_2O = 3CaO{\cdot}Al_2O_3{\cdot}\ CaCl_2{\cdot}10H_2O + Mg(OH)_2.$$

Also, a semiquantitative X-ray diffraction analysis was carried out for specimens consisting of fly ash, MS, and the magnesium chloride additive, which were previously tested for strength (see Table 6). The XRD results are shown in Fig. 4, 5, and Table 8.

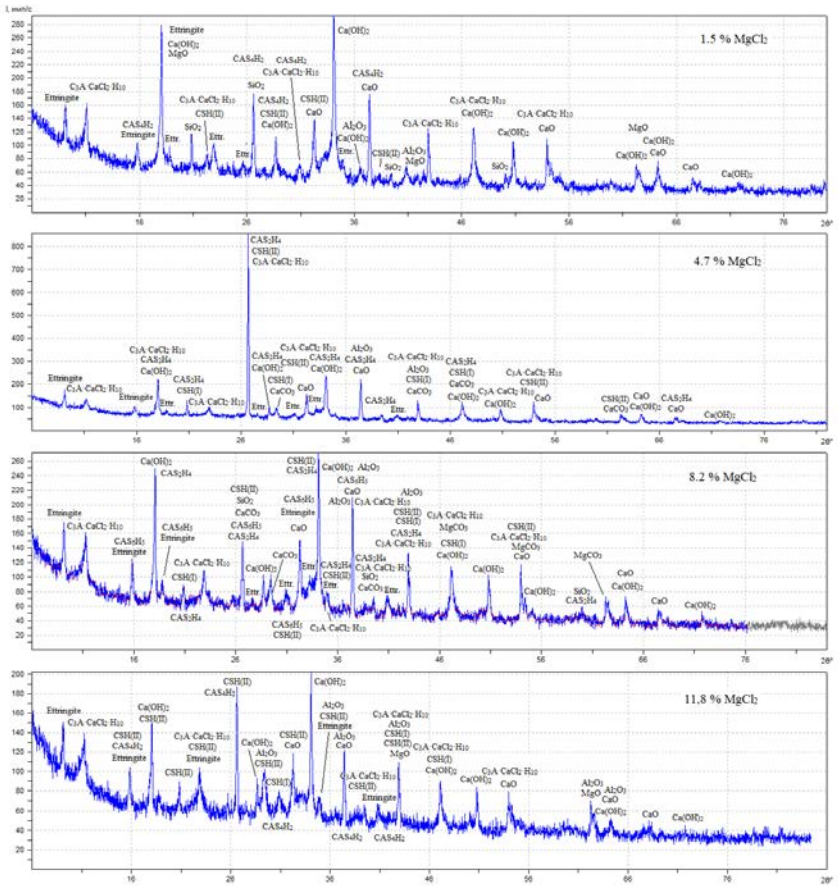

Figure 6. X-ray patterns of specimens with $MgCl_2$ additive, curing in dry (isolated) conditions, after their strength test at the age of 7 days (Table 5).

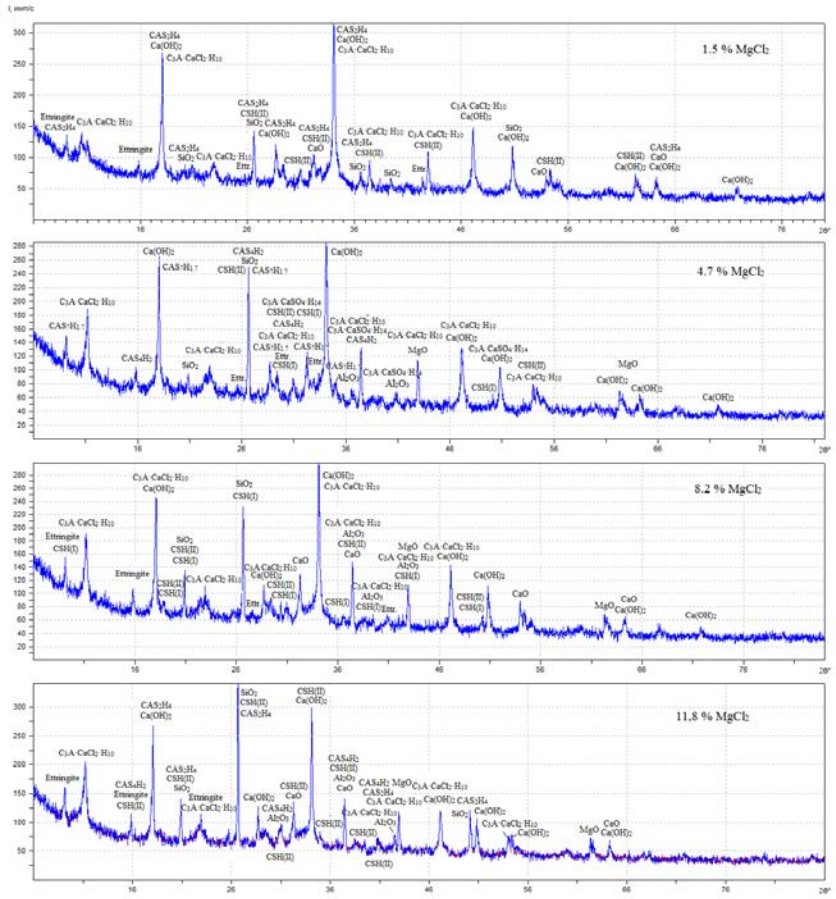

Figure 7. X-ray patterns of specimens with $MgCl_2$ additive, curing in water, after their strength test at the age of 7 days (Table 4).

Table 8. Conventional values of percentage of identified phases.

Phases	Chemical Compound	Curing	Content of $MgCl_2$, % by weight of fly ash			
			1.5	4.7	8.2	11.8
Portlandite	$Ca(OH)_2$	dry	52.6	26.0	31.8	37.2
		in water	70.2	32.9	36.1	42.9
Lime	CaO	dry	23.7	21.7	20.9	17.5
		in water	11.0	14.3	17.7	21.5
Calcium Aluminum Oxide Chloride Hydrate	$C_3A{\cdot}CaCl_2{\cdot}H_{10}$	dry	6.0	3.5	18.3	19.4
		in water	3.9	21.1	14.7	6.1
Calcium Aluminum Hydroxide Hydrate	C_4AH_{13}	dry	8.7	-	-	-
		in water	-	-	-	-
Calcium Aluminum Silicate Hydrates	CAS_xH_y	dry	7.0	34.5	24.2	16.8
		in water	12.7	31.1	26.8	11.7
Calcium Silicate Hydrate	CSH(II)	dry	2.0	14.2	4.9	9.2
		in water	2.2	0.7	4.7	18.3

The main phases identified in the specimens (Table 8) are lime, calcium hydroxide, calcium hydrochloraluminate, and a significant amount of calcium aluminosilicates of the composition CAS_2H_4, CAS_4H_2, CAS_6H_5, $CAS_7H_{1,7}$, which in Table 5 are denoted by the general formula CAS_xH_y. The effect of $MgCl_2$ on other compounds' content manifests differently depending on the concentration. The content of $Ca(OH)_2$ decreases by almost 2 times with an increase in the content of $MgCl_2$ from 1.5 to 4.7 % by weight of fly ash, both in dry and water curing of specimens. At the same time, the content of calcium hydroaluminosilicates increased 5 times during dry hardening and 2.5 times during water hardening. The content of $C_3A{\cdot}CaCl_2{\cdot}H_{10}$ in this range of magnesium chloride concentrations decreased from 6 to 3.5 % during dry curing, and, on the contrary, it increased from 3.9 to 21.1 % during water curing. With a further

increase in the concentration of $MgCl_2$ from 4.7 to 11.8 %, the content of $Ca(OH)_2$ moderately increases, and the content of calcium aluminosilicates decreases for both hardening methods. The calcium hydrochloraluminate formation increases significantly with an increase in the concentration of $MgCl_2$ during dry curing but decreases when the specimens are placed in water. The residual amount of lime can be a little dependent on the $MgCl_2$ content and hydration conditions. Thus, the magnesium chloride assistive promotes the formation of calcium hydrochloraluminate and the redistribution of free lime towards the formation of calcium hydroaluminosilicates instead of $Ca(OH)_2$.

3.3.2. Results of differential thermal analysis

Differential thermal analysis data confirm the XRD results. DTA curves for mixes 2 and 3 at different ages (Table 4) are shown in Fig. 8.

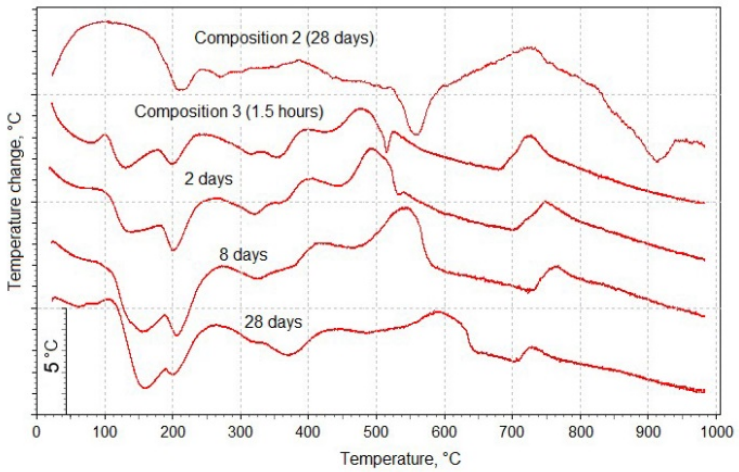

Figure 8. DTA curves of specimens from mixes 2 (without $MgCl_2$ additive) and 3 with 11.8% $MgCl_2$ additive at different ages.

The thermogram of mix 2 shows 3 pronounced endothermic peaks at 210, 560, and 915 °C. The first of them may correspond to the loss of interlayer water in the tobermorite. The effects at 560 and 915 °C refer to the decomposition of $Ca(OH)_2$ and $CaCO_3$, respectively. Other thermograms show several effects caused by $MgCl_2$ influence. These are endothermic peaks with increasing intensity as the specimens' curing period increases, in the temperature range of 130–160 °C. In this temperature range, adsorbed and hydrosilicates and AFm-phases usually lose interlayer water. Thus, $MgCl_2$ promotes the formation of these phases, which also follows from the XRD results. The endothermic peak at 200 °C noted on all thermograms can be attributed to C_4AH_{13}, which is stable in $Ca(OH)_2$ solutions at CaO concentrations higher than 1.08 g/L. This effect may also be associated with dehydrating the CAS_2H_4 compound or other calcium alumina hydrosilicates.

The endothermic effect at 320°C is associated with the presence of C_3AH_6, and the effect at 360 °C is associated with the dehydration of C_3ASH_4. A wide depression in the temperature range of 400–500 °C, shifting to the right with the age of the specimens, presumably indicates the presence of calcium hydrosilicates with a $CaO:SiO_2$ ratio of more than 1,3.

The formation of $C_3A{\cdot}CaCl_2{\cdot}H_{10}$ in this system can be evidenced by endothermic effects at 155, 200–210, and 320 °C. Literature data show similar temperature peaks for this compound. The thermogram of the synthesized calcium hydrochloraluminate [44] shows endothermic peaks at 215 and 330 °C. In work [45], three endothermic peaks were found for the Friedel salt obtained due to hydrothermal synthesis: the peak at 35 °C is due to a structural transition, the peak at 155 and 340 °C corresponds to the loss of interlayer water and hydroxyl condensation, respectively.

The thermograms of mix 3 (Fig. 8) show two exothermic peaks. The first one, with an increase in the age of the specimens, shifts towards a higher temperature, from 475 to 590 °C, and is superimposed on the effect of $Ca(OH)_2$ dehydration, overlapping the heat costs for the decomposition of portlandite. Since mix 2 did not show a similar effect, the addition of $MgCl_2$ can be considered responsible for it. Unfortunately, it has not yet been possible to decipher this effect. The second exothermic peak at 725–765 °C is characteristic of all thermograms, including mix 2 without $MgCl_2$ addition. The most probable in this case is the burnout of unburned carbon particles.

The thermograms shown in Fig. 9 characterize the effect of the magnesium chloride amount on the phase composition of the fly ash – silica fume specimens.

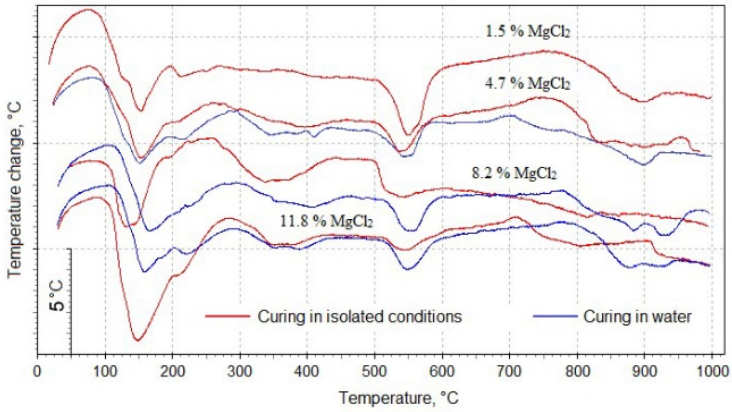

Figure 9. DTA curves of specimens with different MgCl2 content.

As can be seen from Fig. 9, the obtained DTA curves basically repeat the shape of the previous thermograms. That is, in qualitative terms, we have the same data as in the analysis of Fig. 6. It is noteworthy here that with an increase in the $MgCl_2$ content, the depth of the endothermic peak at 150 °C sharply increases, which once again confirms the intensive growth of aluminate hydrates and calcium aluminosilicates in the presence of $MgCl_2$. In this case, the amount of $Ca(OH)_2$ formed decreases, as evidenced by the decreasing depth of the endothermic peak at 550 °C. This is more pronounced during dry curing of the specimens.

3.4. Influence of magnesium chloride on heat generation of fly ash-silica fume binder

The heat generation of the mortar (binder + polyfraction standard sand) per 1 kg of fly ash at a temperature of 20 °C, depending on the mix, is shown in Fig. 10.

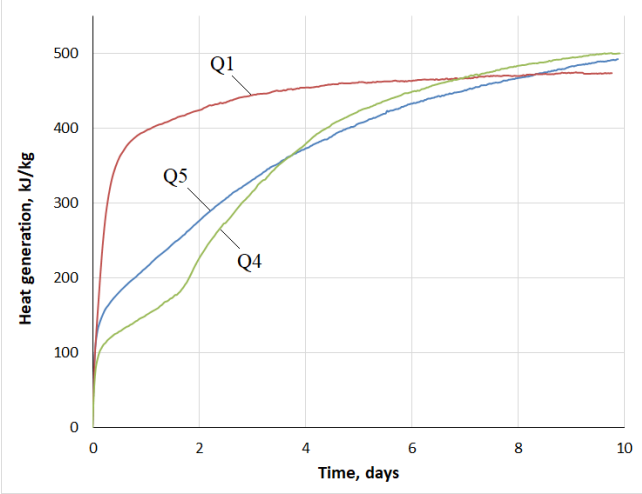

Figure 10. Heat generation of fly ash mortar per 1 kg of fly ash at temperature of 20 °C, depending on the mix: Q1 is without additives; Q4 is with additive of 42.9 % MS; Q5 is with additives of 42.9% MS and 11.8 % $MgCl_2$.

Pure fly ash (curve Q1) reacted very violently with water due to the slaking of free lime. Approximately 1 day after the intense heat release, the process slowed down sharply and ended by the fourth day. In the presence of silica fume (curve Q4), a sharp slowdown of the heat release process was observed. By the end of the second day, the reaction rate increased again, and on the 10th day, the heat release was higher than that of pure fly ash. The addition of $MgCl_2$ compensated for the retarding effect of silica fume and increased the heat release in the first 3 days, giving a smoother curve with a moderate increase in exotherm. Starting from day 4, the heat release curves for the mixes Q4 and Q5 were parallel and very close to each other, with a slight excess of the mix Q4 over Q5. By the end of the experiment, the mix Q5 also overtaked pure fly ash in terms of the total thermal effect.

The heat of hydration experiments require a certain amount of time to prepare the mix and the specimens. In our case, this time was about 30 min. Additional tests were carried out to determine the heating in the first hour of hydration. The mixes of the test are given in Table 9.

Table 9. Test mixes for determining the temperature in the initial period of hydration.

Component	Material Consumption [kg/m^3]		
	t1	t2	t3
Fly ash from Berezovskaya TPP	30	30	30
Silica fume MKU-85	-	12.9 (42.9 %)	12.9 (42.9 %)
$MgCl_2$ (dry)	-	-	3.54 (11.8 %)
Water	19.5	27.9	30.2
Total	49.5	70.8	76.64

Fly ash or a thoroughly mixed fly ash and MS were placed at the bottom of the Dewar flask. The $MgCl_2$ additive was introduced in the paste with mixing water. A closed container with water or an additive solution, suspended on a thin thread, was placed above the dry mixture inside a Dewar flask. The water-solid ratio was 0.65. A closed thermos and a glass thermometer with a division value of 0.1 °C were kept for 1 day in a room with a constant temperature. Before the start of the experiment, the temperature of the dry mix in a thermos was measured and taken as the initial temperature of the specimens. The dry mix in a thermos was closed with prepared water and quickly stirred with the end of a thermometer, fixing the temperature. The first reading was taken 30 s after the moment of shuttering. Each composition was tested twice, and the average value was taken. The results of measuring the temperature of the fly ash-silica fume paste are shown in Fig. 11.

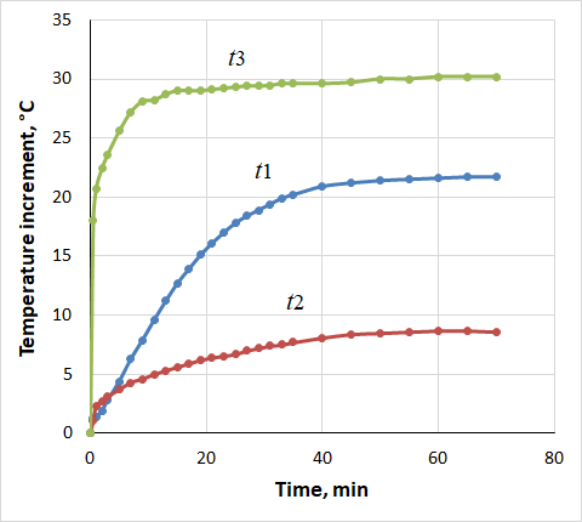

Figure 11. Temperature increment of specimens depending on mix: t1 is fly ash without additives; t2 is fly ash with addition of 42.9% MS; t3 is fly ash with additions of 42.9% MS and 11.8 $MgCl_2$%.

Fig. 11 shows that the temperature of the fly ash (mix t1) for 1 hour of hydration increased by 21.6 °C against the initial one. In the presence of silica fume (mix t2), the hydration rate decreased sharply, and the temperature of the paste increased only by 8.7 °C. Here, the same regularity of the silica fume influence was observed as in the initial period of hardening of the mortar (Fig. 10). Such an effect of silica fume was explained by a decrease in the transfer rate in solutions [46]. The introduction of the $MgCl_2$ additive resulted in an extremely sharp temperature jump in the first seconds after mixing. The temperature increase after 30 s was 18 °C, and after 10 min was 28.2 °C.

This characterizes magnesium chloride as a powerful early strength agent of fly ash-silica fume binder.

3.5. Effect of magnesium chloride on the mortar strength

The specimens consisting of fly ash, silica fume, polyfraction standard sand, and magnesium chloride (Table 5) tested for heat release were also tested for compressive strength at the age of 28 days. Specimens of a cubic form, in 3 pieces per test, had dimensions of 7×7×7 cm. The specimens were stored in a laboratory room with a temperature of (20 ± 2) °C, for the first 7 days in covered forms and the rest of the time in a desiccator above water. Testing hydraulic press PGM-50MG4 with a maximum force of 50 kN was used for testing. During the test, the loading rate was maintained (50±10) kPa/s.

The results of determining the compressive strength of the specimens are shown in the diagram in Fig. 12.

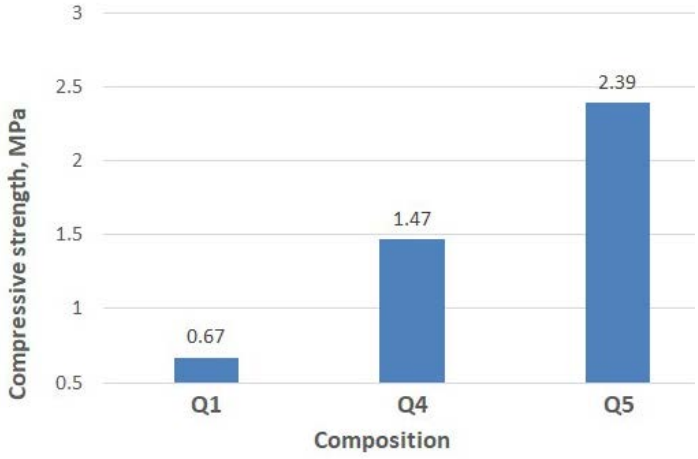

Figure 12. Compressive strength test results of specimens.

From Fig. 12, it can be seen that adding silica fume to the fly ash increased the strength of the specimens by more than 2 times, and adding $MgCl_2$ increased the strength by another 63 %. Authors [36] also obtained greater strength of specimens based on cement and fly ash at high dosages of $MgCl_2$ additive.

The low strength of the tested compositions of the mortar; however, it must be borne in mind that the binder-sand ratio in these solutions ranges from 1:5 to 1:7.

4. Conclusions

This paper presented the results of an experimental studies conducted to evaluate the influence of magnesium chloride additive on a cementless binder consisting of high-calcium fly ash and silica fume. The following key conclusions were drawn from this study:

1. Silica fume added to the high-calcium fly ash of Berezovskaya thermal power plant in an amount of about 40 % eliminates its expansion due to CaO hydration. A mix of fly ash and silica fume exhibits the properties of a binder. Early strength agents can significantly increase the binder strength. However, some agents restore the fly ash expansion despite the silica fume presence.

Of the early strength agents tested, magnesium and calcium chloride showed virtually no expansion, and $MgSO_4$ showed expansion within the normal range for Portland cement. The highest compressive strength of these three additives was provided by $MgCl_2$ (15.2 MPa at the age of 7 days with an additive content of 11.8 %).

2. X-ray Diffraction Analysis showed the following results:

2.1. The interaction of pure fly ash with water in 28 days leads to complete hydration of CaO_{free}. In this case, calcium hydroxide is formed in most hydration products. C_3AH_6 is present in calcium hydroaluminates. The addition of silica fume to the fly ash slows down the hydration of lime. After 28 days of hydration, a significant amount of unreacted CaO_{free} (about 20 %) still remains in the fly ash, and the content of $Ca(OH)_2$ is almost halved.

2.2. The effect of $MgCl_2$ was investigated for three hydration periods. After 1.5 hours, a significant amount of unreacted CaO_{free} (36 %) and, accordingly, a small amount of $Ca(OH)_2$ remain in the composition of the binder. In subsequent periods, the content of lime decreases, and by 8 days, it is completely bound into hydrates, aluminates, and calcium aluminosilicates, which make up a significant proportion of the total number of neoplasms. The XRD results show that $MgCl_2$ accelerates the hydration of lime and its binding to silica. At the same time, the addition of magnesium chloride intensifies the processes of formation of crystalline hydrates of calcium aluminosilicates.

With the introduction of $MgCl_2$, calcium hydrochloraluminate (Friedel's salt) is formed, which has not previously been observed in the composition of the hydration products of the binder. The content of $3CaO{\cdot}Al_2O_3{\cdot}CaCl_2{\cdot}10H_2O$ changes little with the age of the specimens.

2.3. The main phases identified in specimens consisting of fly ash, silica fume, and different $MgCl_2$ content at the age of 9 days are lime, calcium hydroxide, calcium hydrochloraluminate, and a significant amount of calcium aluminosilicates of the composition CAS_2H_4, CAS_4H_2, CAS_6H_5, $CAS_7H_{1,7}$. The effect of $MgCl_2$ on other compounds' content manifests differently depending on the concentration. The content of $Ca(OH)_2$ decreases by almost 2 times, both during dry and water curing of specimens, if the $MgCl_2$ content increases from 1.5 to 4.7 % by weight of fly ash. This is accompanied by a sharp increase in the amount of calcium hydroaluminosilicates. With a further increase in the $MgCl_2$ content from 4.7 to 11.8 %, the $Ca(OH)_2$

content increases moderately, and the content of calcium aluminosilicates decreases. The calcium hydrochloraluminate formation increases significantly with an increase in the concentration of $MgCl_2$ during dry curing but decreases when the specimens are placed in water. Thus, the magnesium chloride promotes the calcium hydrochloraluminate formation and the redistribution of free lime towards the formation of calcium hydroaluminosilicates instead of $Ca(OH)_2$.

3. In the DTA curves, with an increase in the $MgCl_2$ content, the depth of the endothermic peak at 150 °C increases sharply, which confirms the intensive growth of aluminate hydrates and calcium aluminosilicates in the presence of $MgCl_2$.

4. Pure fly ash reacts very violently with water due to the slaking of free lime. During the first day, 85 % of the heat is released from the final total value of the released heat in the experiment for 10 days. There is a sharp slowdown in the process of heat release in the presence of silica fume in the initial period of hardening. The thermal effect was only 30% of the final value by the end of the first day. The addition of $MgCl_2$ partially compensates for the retarding effect of silica fume. In this case, 44 % of the heat from the final value is released during the first day. It should be noted that the final value of the total heat release is approximately the same in all three cases.

5. The addition of $MgCl_2$ to the mortar with polyfraction standard sand increases the compressive strength by 63 %.

References

1. Petrov, V.V., Protsenko, A.E., Sapozhnik, K.R. Solid-cabide tool waste recycling technology. Construction Materials and Products. 2022. 5(3). Pp. 27–34. DOI: 10.58224/2618-7183-2022-5-3-27-34
2. Zakrevskaya, L.V., Gavrilenko, A.A., Kapush, I.R., Lyubin, P.A. Creating ground concrete and strengthening substrates using mining waste. Construction Materials and Products. 2022. 5 (3). Pp. 35–44. DOI: 10.58224/2618-7183-2022-5-3-35-44
3. Kashapov, R.N., Kashapov, N.F., Kashapov, L.N., Klyuev, S.V., Chebakova, V.Yu. Study of the plasma-electrolyte process for producing titanium oxide nanoparticles. Construction Materials and Products. 2022. 5 (5). Pp. 70–79. DOI: 10.58224/2618-7183-2022-5-5-70-79
4. Kashapov, R.N., Kashapov, N.F., Kashapov, L.N., Klyuev, S.V. Plasma electrolyte production of titanium oxide powder. Construction Materials and Products. 2022. 5 (6). Pp. 75–84. DOI: 10.58224/2618-7183-2022-5-6-75-84
5. Vatin, N., Barabanshchikov, Yu., Usanova, K., Akimov, S., Kalachev, A., Uhanov, A. Cement-based materials with oil shale fly ash additives. IOP Conf Ser Earth Environ Sci. IOP Publishing Ltd. 2020. 578 (1). Article no. 012043. DOI: 10.1088/1755-1315/578/1/012043
6. Barabanshchikov, Yu., Usanova, K., Akimov, S., Uhanov, A. Influence of Electrostatic Precipitator Ash “Zolest-Bet” and Silica Fume on Sulfate Resistance of Portland Cement. Materials. 2020. 13(21). Article no. 4917. DOI: 10.3390/ma13214917
7. Barabanshchikov, Y., Usanova, K. Influence of High-Calcium Oil Shale Ash Additive on Concrete Properties. Lecture Notes in Civil Engineering. 2021. 150 LNCE. Pp. 23–34. DOI: 10.1007/978-3-030-72404-7_3
8. Raju, S., Rathinam, J., Dharmar, B., Rekha, S., Avudaiappan, S., Amran, M., Usanova, K., Fediuk, R., Guindos, P., Ramamoorthy, R.V. Cyclically Loaded Copper Slag Admixed Reinforced Concrete Beams with Cement Partially Replaced with Fly Ash. Materials. MDPI. 2022. 15(9). Article no. 3101. DOI: 10.3390/ma15093101
9. Teixeira, E.R., Mateus, R., Camoes, A., Braganca, L., Branco, F.G. Comparative environmental life-cycle analysis of concretes using biomass and coal fly ashes as partial cement replacement material. Journal of Cleaner Production. 2016. 112. Pp. 2221–2230. DOI: 10.1016/j.jclepro.2015.09.124
10. Amran, M., Fediuk, R., Murali, G., Avudaiappan, S., Ozbakkaloglu, T., Vatin, N.I., Karelina, M., Klyuev, S., Gholampour, A. Fly ash-based eco-efficient concretes: A comprehensive review of the short-term properties. Materials. 2021. 14(15). Article no. 4264. DOI: 10.3390/ma14154264
11. Öz, H.Ö., Yücel, H., Güneş, M., Köker, T. Fly-ash-based geopolymer composites incorporating cold-bonded lightweight fly ash aggregates. Construction and Building Materials. 2021. 272. Pp. 121963. DOI: 10.1016/j.conbuildmat.2020.121963
12. Narattha, C., Chaipanich, A. Effect of curing time on the hydration and material properties of cold-bonded high-calcium fly ash–Portland cement lightweight aggregate. Journal of Thermal Analysis and Calorimetry. 2021. 145(17). Pp. 2277–2286. DOI: 10.1007/s10973-020-09730-8
13. Yang, S., Zhao, R., Ma, B., Si, R., Zeng, X. Mechanical and fracture properties of fly ash-based geopolymer concrete with different fibers. Journal of Building Engineering. 2023. 63. Part A. Article no. 105281. DOI: 10.1016/j.jobe.2022.105281
14. Korniejenko, K., Łach, M., Marczyk, J., Ziejewska, C., Halyag, N.P., Mucsi, G. Fly ash as a raw material for geopolymerisation-mineralogical composition and morphology. IOP Conf Ser Mater Sci Eng. 2019. 706(1). Article no. 012006. DOI: 10.1088/1757-899X/706/1/012006
15. Anees Ahmed, A.A., Lesovik, R., Lesovik, V., Fediuk, R., Klyuev, R., Amran, M., Ali, M., de Azevedo, A.R.G., Vatin, N. Demolition Waste Potential for Completely Cement-Free Binders. Materials. 2022. 15(17). Article no. 6018. DOI: 10.3390/ma15176018
16. Salamanova, M., Murtazaev, S.-A., Saidumov, M., Alaskhanov, A., Murtazaeva, T., Fediuk, R. Recycling of Cement Industry Waste for Alkali-Activated Materials Production. Materials. 2022. 15. Article no. 6660. DOI: 10.3390/ma15196660
17. Xu, G., Shi, X. Characteristics and applications of fly ash as a sustainable construction material: A state-of-the-art review. Resources, Conservation and Recycling. 2018. 136. Pp. 95–109. DOI: 10.1016/j.resconrec.2018.04.010
18. Zhang, N., Yu, H., Gong, W., Liu, T., Wang, N., Tan, Y., Wu, C. Effects of low- and high-calcium fly ash on the water resistance of magnesium oxysulfate cement. Construction and Building Materials. 2020. 230. Article no. 116951. DOI: 10.1016/j.conbuildmat.2019.116951
19. Fan, W.J., Wang, X.Y., Park, K.B. Evaluation of the Chemical and Mechanical Properties of Hardening High-Calcium Fly Ash Blended Concrete. Materials. 2015. 8(9). Pp. 5933–5952. DOI: 10.3390/ma8095282

20. Goenawan, V., Antoni, A., Hardjito D. A Preliminary Study on Cracking Tendency of Cement Paste Incorporating High Calcium Fly Ash. Applied Mechanics and Materials. 2015. 815. Pp. 158–163. DOI: 10.4028/www.scientific.net/AMM.815.158
21. Dhole, R., Thomas, M.D.A., Folliard, K., Drimalas, T. Sulfate resistance of mortar mixtures of high-calcium fly ashes and other pozzolans. ACI Mater Journal. 2011. 108(6). Pp. 645–654.
22. Antiohos, S., Tsimas, S. Investigating the role of reactive silica in the hydration mechanisms of high-calcium fly ash/cement systems. Cement and Concrete Composites. 2005. 27 (2). Pp. 171–181. DOI: 10.1016/j.cemconcomp.2004.02.004
23. Korpa, A., Seiti, B., Xhaxhiu, K., Mele, A., Trettin, R. Processing of high sulphate and free lime calcareous coal fly ash for producing high volume blended cements and complying grade products employed in civil engineering. Zastita materijala. 2014. 55(3). Pp. 251–258. DOI: 10.5937/ZasMat1403251K
24. Tsimas, S., Moutsatsou-Tsima, A. High-calcium fly ash as the fourth constituent in concrete: problems, solutions and perspectives. Cement and Concrete Composites. 2005. 27. 2. Pp. 231–237.
25. Klyuev, S.V., Bratanovskiy, S.N., Trukhanov, S.V., Manukyan, H.A. Strengthening of concrete structures with composite based on carbon fiber. Journal of Computational and Theoretical Nanoscience. 2019. 16(7). Pp. 2810–2814. DOI: 10.1166/jctn.2019.8132
26. Chen, B., Liu, J. Effect of fibers on expansion of concrete with a large amount of high f-CaO fly ash. Cement and Concrete Composites 2003. 33(10). Pp. 1549–1552.
27. Klyuev, S.V., Kashapov, N.F., Radaykin, O.V., Sabitov, L.S., Klyuev, A.V., Shchekina, N.A. Reliability coefficient for fibreconcrete material. Construction Materials and Products. 2022. 5 (2). Pp. 51–58. DOI: 10.58224/2618-7183-2022-5-2-51-58
28. Anthony, E.J., Bulewicz, E.M., Dudek, K., Kozak, A. The long term behaviour of CFBC ash–water systems. Waste Management. 2002. 22(1). Pp. 99–111. DOI: 10.1016/s0956-053x(01)00059-9.
29. Blondin, J., Iribarne, A., Iribarne, J., Anthony, E.J. Hydration of combustion ashes — a chemical and physical study. Fuel. 2001. 80(6). Pp. 773–784.
30. Sheng, G., Li, Q., Zhai, J., Li, F. Self-cementitious properties of fly ashes from CFBC boilers co-firing coal and high-sulphur petroleum coke. *Cement and Concrete Research.* 2007. 37(6). Pp. 871–876. DOI: 10.1016/j.cemconres.2007.03.013
31. Domanskaya, I., Oleynik, V., Minyazev, D. ICSC Problems and Perspectives of high-calcium fly ash from heat power plants in the composition of “green” building materials. E3S Web of Conferences. 2016. 6. Article no. 01014. DOI: 10.1051/e3sconf/20160601014
32. Barabanshchikov, Y., Usanova, K. Influence of Silica Fume on High-Calcium Fly Ash Expansion during Hydration. Materials. 2022. 15(10). Article no. 3544. DOI: 10.3390/ma15103544
33. Li, Z., Lu, D., Gao, X. Analysis of correlation between hydration heat release and compressive strength for blended cement pastes. Construction and Building Materials. 2020. 260. Article no. 120436. DOI: 10.1016/j.conbuildmat.2020.120436
34. Ghadir, P., Razeghi, H.R. Effects of sodium chloride on the mechanical strength of alkali activated volcanic ash and slag pastes under room and elevated temperatures. Construction and Building Materials. 2022. 344(2). Article no. 128113. DOI: 10.1016/j.conbuildmat.2022.128113
35. Li, J., Huang, Ya., Li, W., Guo, Ya., Ouyang, Sh., Cao, G. Study on dynamic adsorption characteristics of broken coal gangue to heavy metal ions under leaching condition and its cleaner mechanism to mine water. Journal of Cleaner Production. 2021. 329. Article no. 129756. DOI: 10.1016/j.jclepro.2021.129756
36. Chen, S., Du, Z., Zhang, Z., Zhang, H. Effects of chloride on the early mechanical properties and microstructure of gangue-cemented paste backfill. Construction and Building Materials. 2020. 235. Article no. 117504. DOI: 10.1016/j.conbuildmat.2019.117504
37. Ouyang, S., Huang, Y., Wu, L., Yin, W., Yang, x., Wang, J., Wang, G., Li, J., Lei, Y. Effects of chlorides on setting time, hydration heat and hydration products of fresh slurry of cemented paste backfill. Case Studies in Construction Materials. 2022. 17. Article no. e01462. DOI: 10.1016/J.CSCM.2022.E01462
38. Khan, I., François, R., Castel, A. Prediction of reinforcement corrosion using corrosion induced cracks width in corroded reinforced concrete beams. Cement and Concrete Research. 2014. 56. Pp. 84–96. DOI: 10.1016/j.cemconres.2013.11.006
39. Cheewaket, T., Jaturapitakkul, C., Chalee, W. Initial corrosion presented by chloride threshold penetration of concrete up to 10 year-results under marine site. Construction and Building Materials. 2012. 37. Pp. 693–698. DOI: 10.1016/j.conbuildmat.2012.07.061
40. Chen, Sh., Shui, Z., Sun, T., Gao, X., Guo, C. Effects of sulfate and magnesium ion on the chloride transportation behavior and binding capacity of Portland cement mortar. Construction and Building Materials. 2019. 204(7). Pp. 265–275. DOI: 10.1016/j.conbuildmat.2019.01.132
41. Shi, Z., Geiker, M.R., Lothenbach, B., De Weerdt, K., Frreiro, S., Enemark-Rasmussen, K., Skibsted, J. Friedel’s salt profiles from thermogravimetric analysis and thermodynamic modelling of Portland cement-based mortars exposed to sodium chloride solution. Cement and Concrete Composites. 2017. 78. Pp. 73–83. DOI: 10.1016/j.cemconcomp.2017.01.002
42. Yuan, Q., Shi, C., De Schutter, G., Audenaert, K. Chloride binding of cement-based materials subjected to external chloride environment – A review. Construction and Building Materials. 2009. 23(1). Pp. 1–13. DOI: 10.1016/j.conbuildmat.2008.02.004
43. Zaporozhets, I.D., Okorokov, S.D., Pariyskiy, A.A. Teplovydeleniye betona [Heat Liberation by concrete]. Moscow: Stroyizdat, 1966. 314 p. (rus)
44. Heller, L., Ben-Yair, M. Effect of chleride solutions on Portland cement. Journal of Applied Chemistry. 1966. 16(8).
45. Rapin, J.Pp., Renaudin, G., Elkaim, E., Francois, M. Structural transition of Friedel’s salt $3CaO{\cdot}Al_2O_3{\cdot}CaCl_2{\cdot}10H_2O$ studied by synchrotron powder diffraction. Cement and Concrete Research. 2002. 32(4). Pp. 513–519. DOI: 10.1016/S0008-8846(01)00716-5
46. Lobo, C., Cohen, M.D. Hydration of type K expansive cement paste and the effect of silica fume: I. Expansion and solid phase analysis. Cement and Concrete Research. 1992. 22(5). Pp. 961–969.

Information about authors:

Kseniia Usanova,
ORCID: https://orcid.org/0000-0002-5694-1737
E-mail: plml@mail.ru

Yuriy Barabanshchikov, *Doctor of Technical Sciences*
ORCID: https://orcid.org/0000-0001-7011-8213
E-mail: ugb@mail.ru

Saurav Dixit,
E-mail: sauravarambol@gmail.com

Received 16.07.2023. Approved after reviewing 22.08.2023. Accepted 23.08.2023.